

Supplementary materials

Natural DNA-Assisted RuP₂ on Highly Graphitic N,P-Codoped Carbon for pH-Wide Hydrogen Evolution

Jingshu Wang, Qian Yu, Haibo Li, Ruiqing Li, Suyuan Zeng, Qingxia Yao, Zengjing Guo, Hongyan Chen, Konggang Qu*

School of Chemistry and Chemical Engineering, Shandong Provincial Key Laboratory/Collaborative Innovation Center of Chemical Energy Storage & Novel Cell Technology, Liaocheng University, Liaocheng 252059, China
Email: qukonggang@lcu.edu.cn

Experimental

Synthesis

The purchased DNA from salmon sperm (ssDNA) was chosen as natural DNA. 300 mg ssDNA was added into 30 mL ultrapure water (18.2 MΩ·cm) with 100 μL 25% ammonia water, 75 mg RuCl₃ was then added after ssDNA dissolving, the mixture was stirred overnight and dried by rotary evaporation. The obtained powder was pyrolyzed under 900 °C for 3 h in a tube furnace with a heating rate of 5 °C min⁻¹ at Ar atmosphere, to obtain RuP₂/NPC. RuP/NPC was prepared at the pyrolysis temperature of 800 °C according to the aforesaid procedure. Meanwhile, adenosine instead of ssDNA, was used to prepare Ru/N-doped carbon (Ru/NC) following the same procedure with RuP₂/NPC.

Characterizations

The morphology and structure was examined by the transmission electron microscope (TEM, Talos F200X G2), powder X-ray diffraction (XRD, SmartLab 9kW) and Raman spectrometer with an excitation wavelength of 532 nm (HORIBA iHR550). The component information were obtained by TEM energy-dispersive X-ray spectroscopy (EDS) mapping and X-ray photoelectron spectroscopy (XPS, Kratos Axis Ultra spectrometer). The specific surface areas were extracted with nitrogen adsorption-desorption isotherm (Micrometrics Tristar II) by the Brunauer-Emmett-Teller (BET) model at a pressure range of P/P₀ = 0.05-0.3, along with the Barrett-Joyner-Halenda (BJH) model for pore size distribution by the adsorption branch on isotherm.

Electrocatalytic experiments

The electrochemical station (Reference 3000, Gamry Instruments, USA) with a rotating disk electrode (RDE) system were used to conduct the electrochemical measurements. For the preparation of working electrode, the samples were initially ultrasonically dispersed into aqueous inks with the concentration of 2 mg mL^{-1} . $20 \mu\text{l}$ of the catalyst ink was dropped onto a pre-prepared RDE with the diameter of 5 mm and dried at ambient condition, then $5 \mu\text{l}$ of 0.5 wt. % Nafion aqueous solution was added to increase the adherence. An Ag/AgCl/KCl (3.5 M) electrode and a graphitic carbon was selected as the reference and counter electrodes, the volume of 100 mL electrolyte was added into a 5-port electrolytic cell with N_2 gas inlet during the tests. The equation $E_{\text{RHE}} = E_{\text{Ag/AgCl}} + (0.205 + 0.059 \text{ pH}) \text{ V}$ was used to calibrate the potentials.

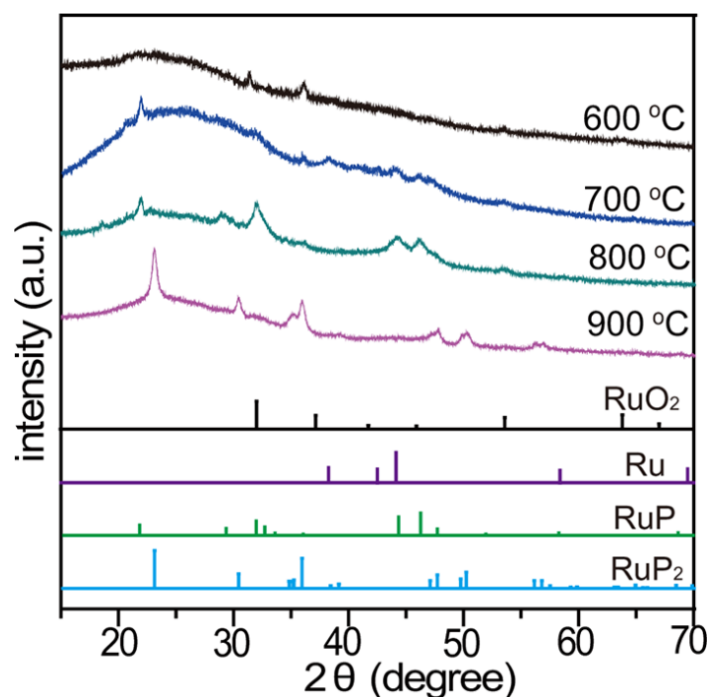


Fig. S1 XRD patterns of the pyrolyzed products at different temperatures.

The evolution of metallic components with the pyrolysis temperature rising from 600 to 900 °C was monitored with XRD. At 600 °C, the diffractive peaks at 31.4° and 36.3° are ascribed to (111) and (200) crystal planes of RuO_2 , but both with obvious peak shift to the left compared with standard 32.1° and 37.2° (JCPDS No.50-1428), maybe due to the doping of larger N and P heteroatoms into the RuO_2 lattice. At 700 °C, the peak at 38.4° corresponds to (100) crystal plane of Ru (JCPDS No.06-0663), while the peaks at 21.7° , 44.2° and 46.1° correspond to (101), (200) and (211) crystal planes of RuP (JCPDS No.65-1863). At 800 °C, a pure RuP phase was observed with stronger

peaks at 21.7 °, 32.1 °, 44.2 ° and 46.1 ° correspond to (101), (200), (112), and (211) crystal planes of RuP. As for 900 °C, the characteristic peaks at 23.0 °, 30.3 °, 35.8 °, 47.5 °, 50.2 ° and 56.3 ° can separately agree with the (110), (020), (101), (121), (211) and (310) crystal planes of RuP₂ (JCPDS No.34-0333).

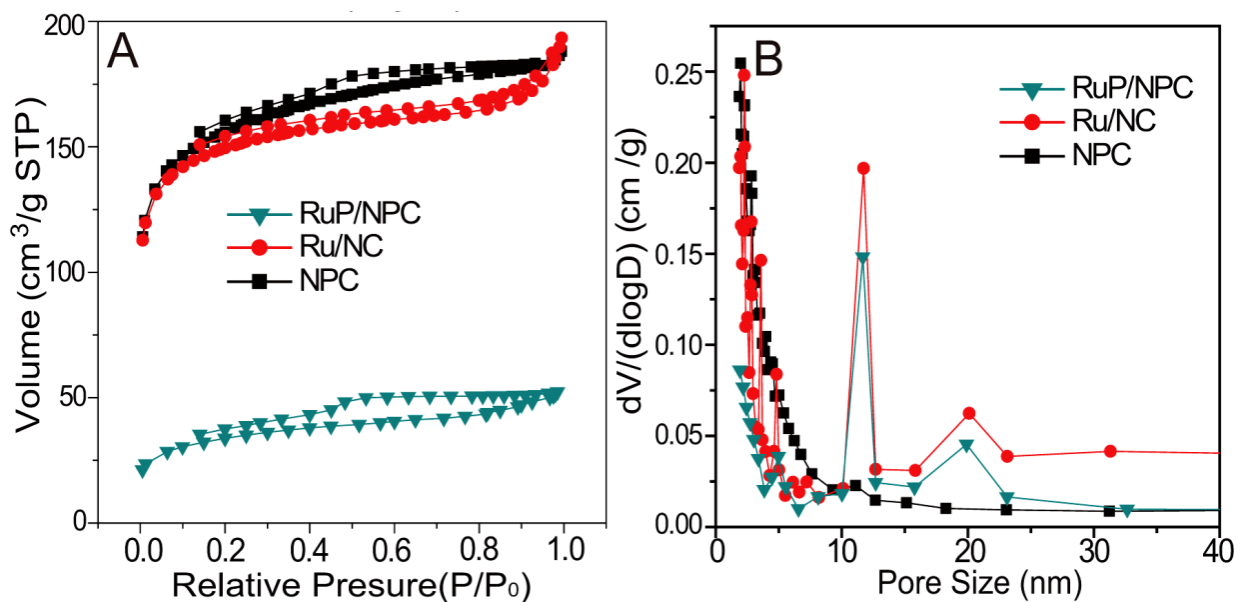


Fig. S2 (A) The N₂ adsorption-desorption isotherms and (B) pore size distribution curves of RuP/NPC, Ru/NC and NPC.

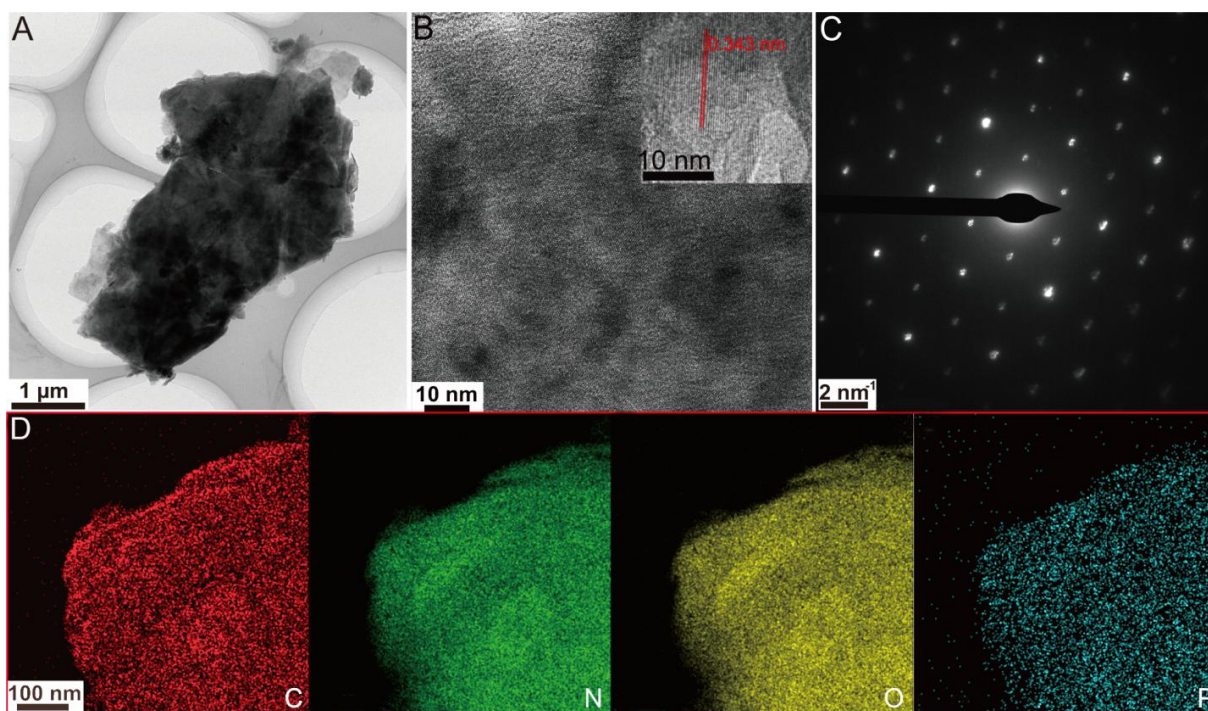


Fig. S3 (A, B) TEM images of NPC at different magnifications, (C) the selected electron diffraction of NPC, (D) TEM elemental mapping images of C, N, O and P elements in NPC.

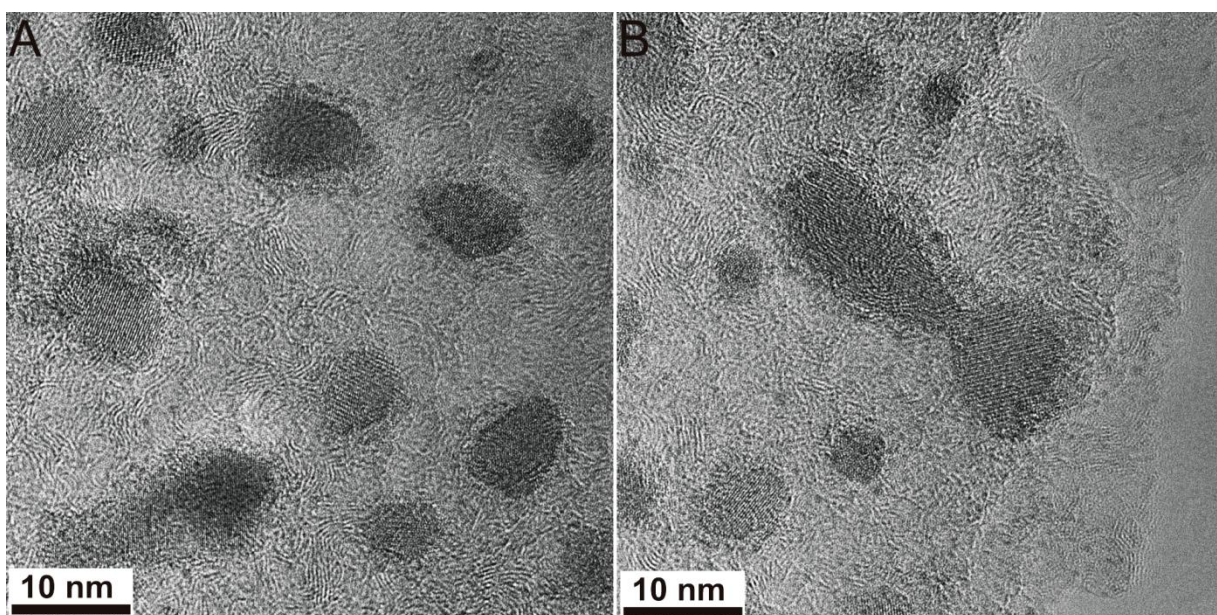


Fig. S4 The high-resolution TEM images of RuP₂/NPC.

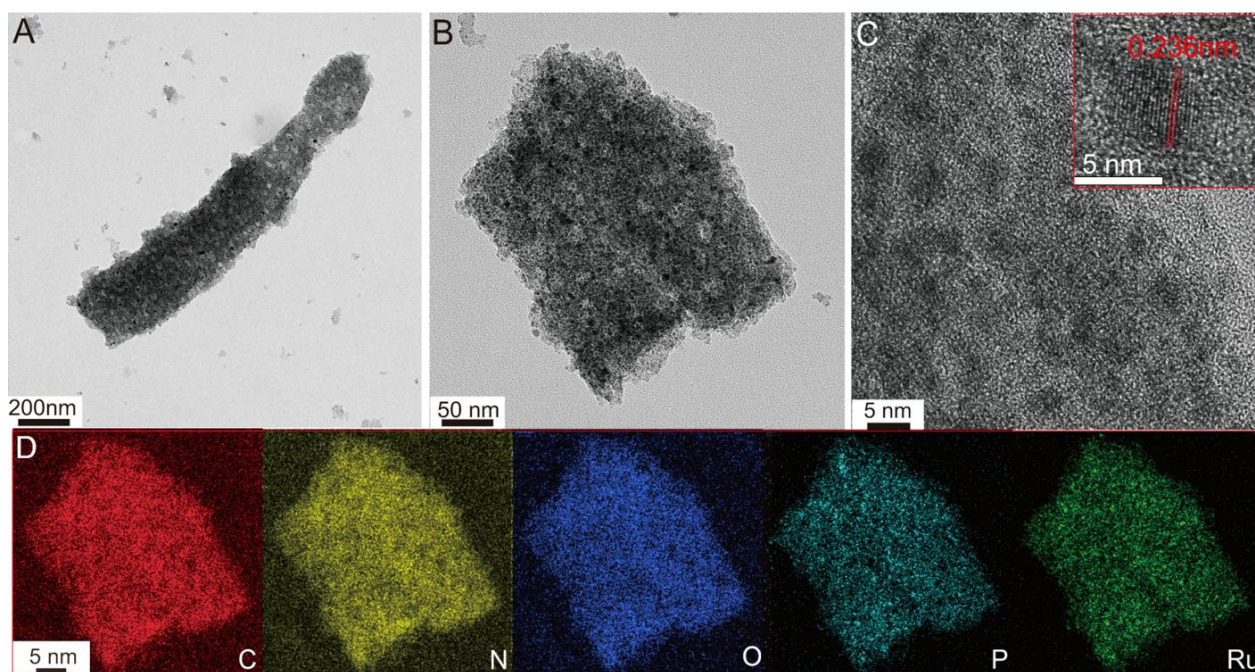


Fig. S5 (A-C) TEM images of RuP/NPC at different magnifications, (D) TEM elemental mapping images of C, N, O, P and Ru elements in RuP/NPC.

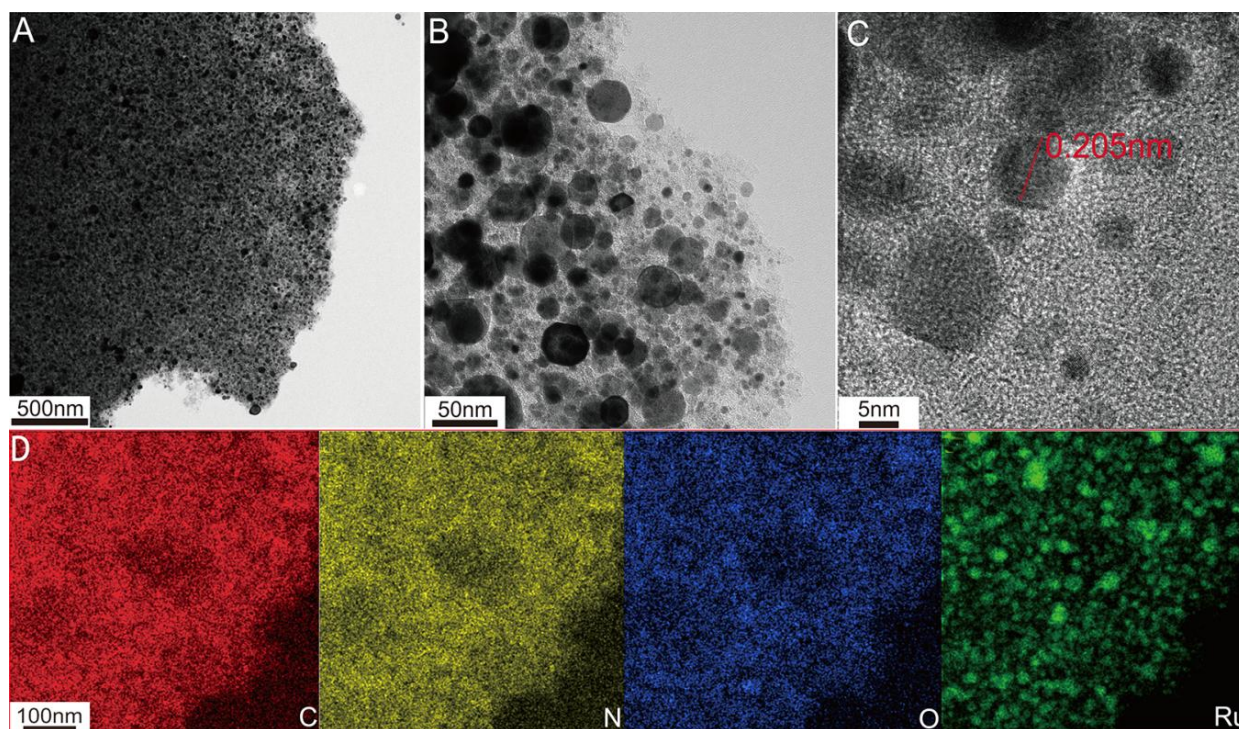


Fig. S6 (A-C) TEM images of Ru/NC at different magnifications, (D) TEM elemental mapping images of C, N, O and Ru elements in Ru/NC.

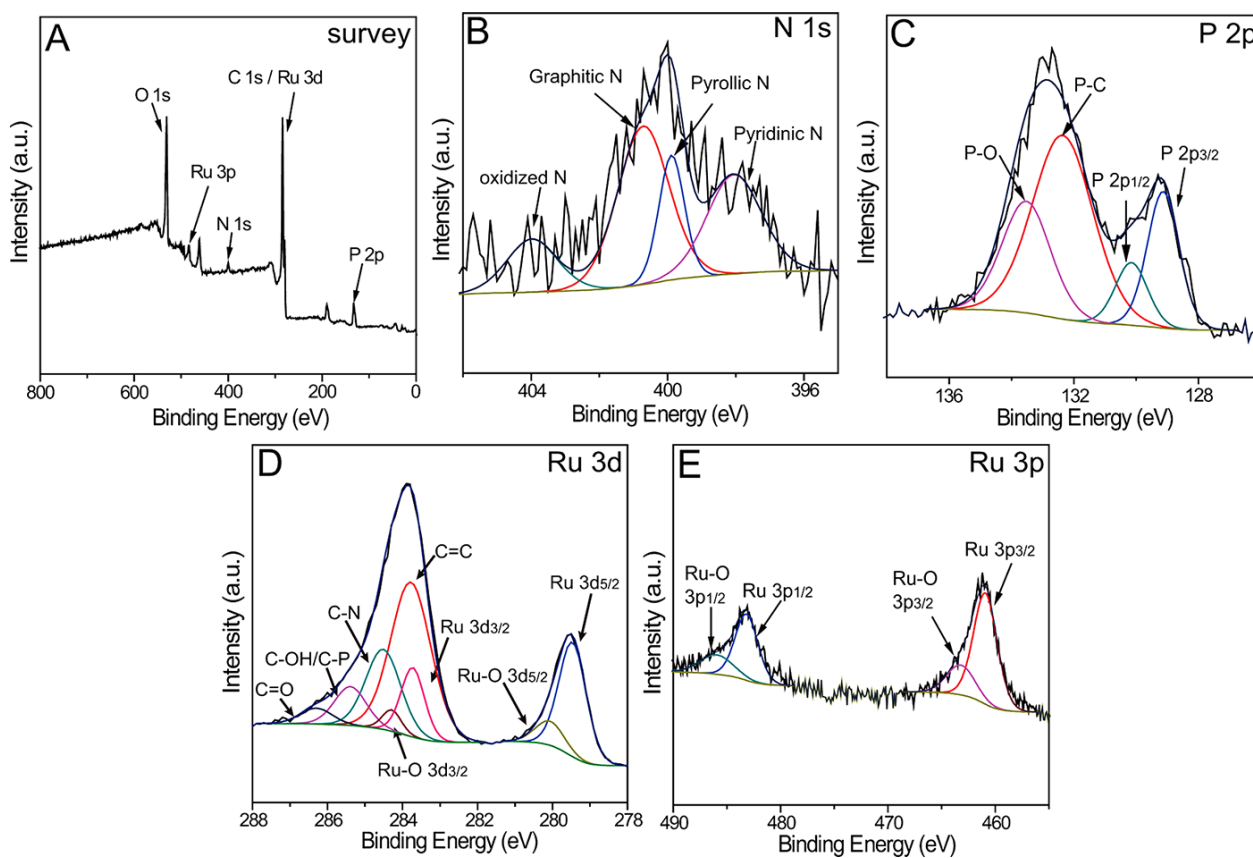


Fig. S7 (A) XPS survey scan and high-resolution XPS spectra of (B) N 1s, (C) P 2p, (D) Ru 3d and (E) Ru 3p of RuP/NPC.

For RuP/NPC, the high-resolution N 1s spectrum can be divided into four subpeaks around 398.0, 399.8, 400.6 and 404.0 eV, which correspond to pyridinic, pyrrolic, graphitic and oxidized N species, respectively. Additionally, the P 2p spectra can be fitted into four peaks, two of which located at around 129.1 and 130.2 eV separately agree with the P 2p_{3/2} and P 2p_{1/2} in RuP₂, and the other centered in 132.4 and 133.5 eV are attributed to the P–C and P–O bonds. The high-resolution XPS regions of Ru 3d overlap with C 1s, the single peak at 279.5 and 280.1 eV are assigned to Ru 3d_{5/2} and Ru-O 3d_{5/2} combined with Ru 3d_{3/2} peak located at 283.6 eV and Ru-O 3d_{3/2} peak at 284.3 eV, meanwhile, the peaks at 283.7, 284.5, 285.4 and 286.3 eV are attributed to C=C, C-N, C-O/C-P, and C=O moieties, respectively. As to XPS region of Ru 3p, the peaks at 460.9 and 463.5 eV are assigned to Ru 3p_{3/2} and Ru-O 3p_{3/2}, combined with Ru 3p_{1/2} peak located at 483.2 eV and Ru-O 3p_{1/2} peak at 486.1 eV.

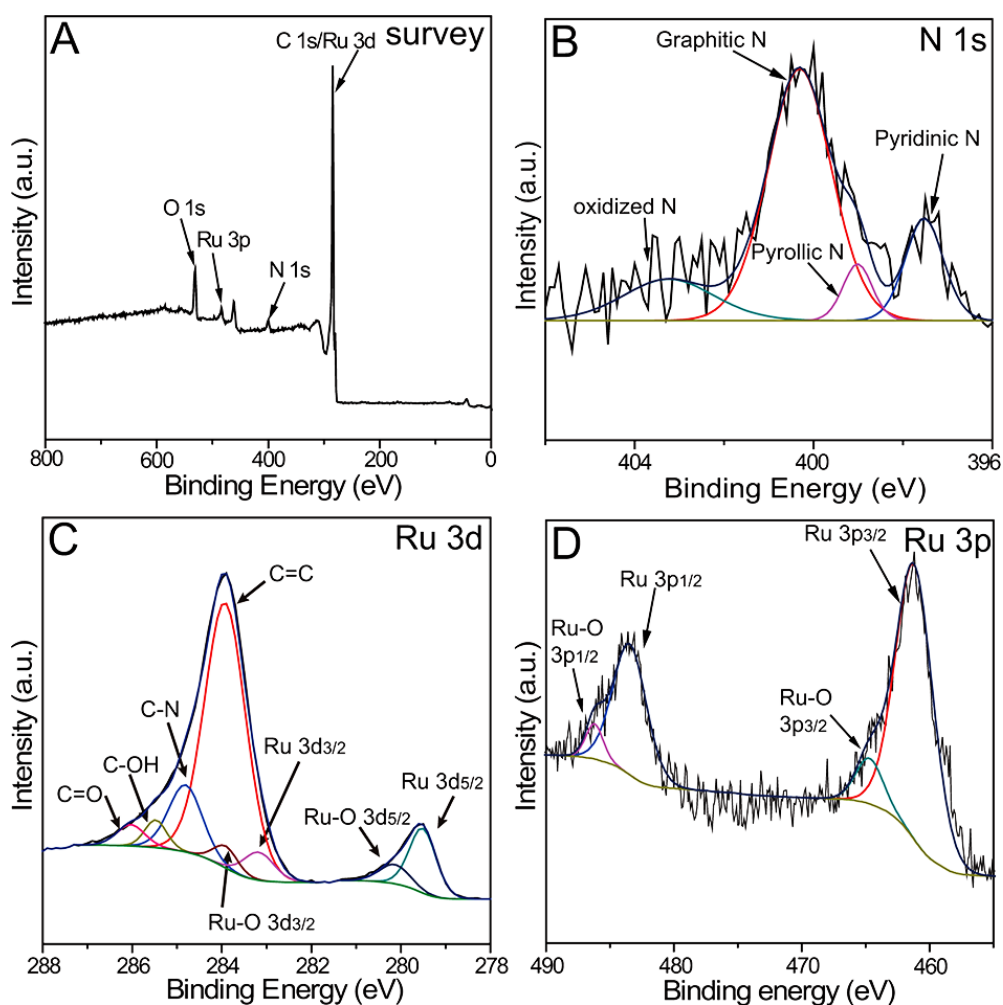


Fig. S8 (A) XPS survey scan and high-resolution XPS spectra of (B) N 1s, (C) Ru 3d and (D) Ru 3p of Ru/NC.

For Ru/NC, the high-resolution N 1s spectrum can be divided into four subpeaks around 397.8, 399.3, 400.3 and 403.3 eV, which correspond to pyridinic, pyrrolic, graphitic and oxidized N species, respectively. Additionally, the high-resolution XPS regions of Ru 3d overlap with C 1s, the peaks at 279.6 and 280.2 eV are assigned to Ru 3d_{5/2} and Ru-O 3d_{5/2}, combined with Ru 3d_{3/2} peak located at 283.2 eV and Ru-O 3d_{3/2} peak at 283.9 eV, meanwhile, the peaks at 283.9, 284.8, 285.5 and 286.0 eV are attributed to C=C, C-N, C-OH and C=O moieties, respectively. As to XPS region of Ru 3p, the peaks at 461.3 and 464.6 eV are assigned to Ru 3p_{3/2} and Ru-O 3p_{3/2}, combined with Ru 3p_{1/2} peak located at 483.5 eV and Ru-O 3p_{1/2} peak at 486.3 eV.

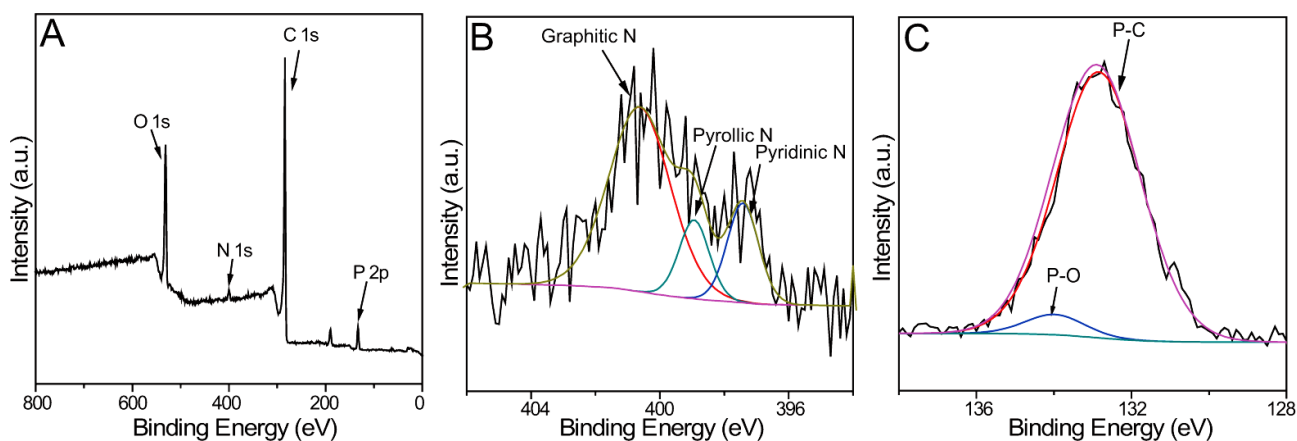


Fig. S9 (A) XPS survey scan and high-resolution XPS spectra of (B) N 1s and (C) P 2p of NPC.

For NPC, the high-resolution N 1s spectrum can be also divided into three subpeaks around 397.7, 399.2 and 400.7 eV, corresponding to pyridinic, pyrrolic and graphitic N species, respectively. The P 2p spectra can be fitted into two peaks centered in 132.7 and 133.9 eV, attributing to the P-C and P-O bonds.

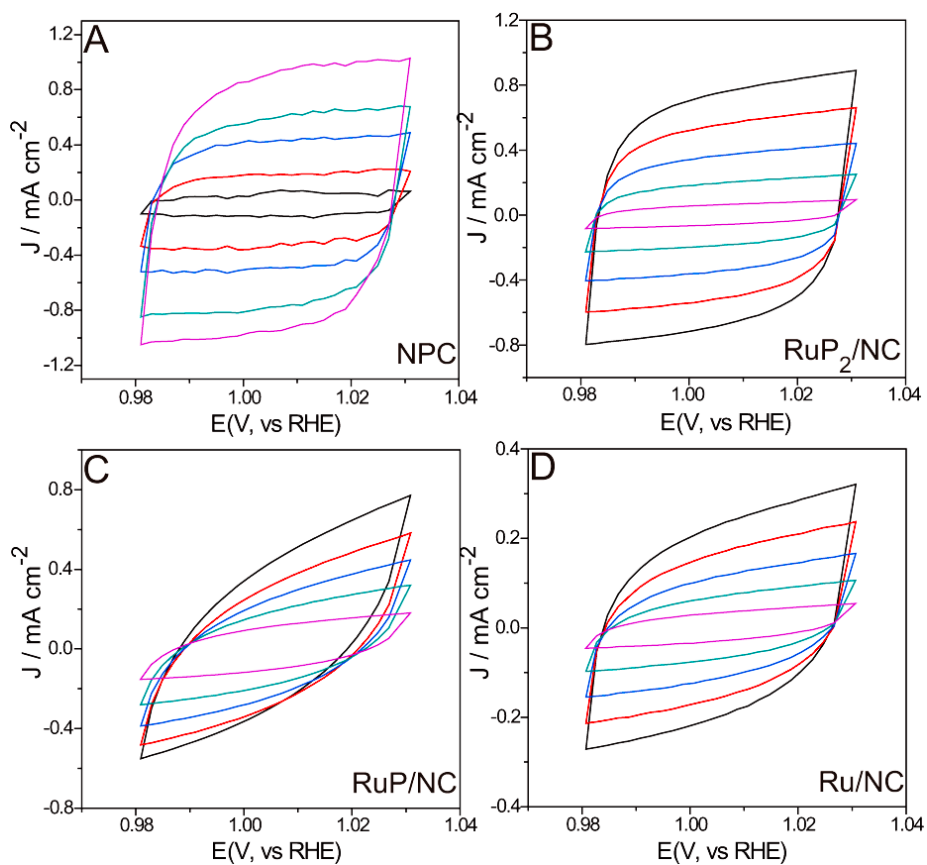


Fig. S10 CV curves at different scan rates (20, 40, 60, 80 and 100 mV s^{-1}) of (A) NPC, (B) RuP_2/NC , (C) RuP/NC and (D) Ru/NC .

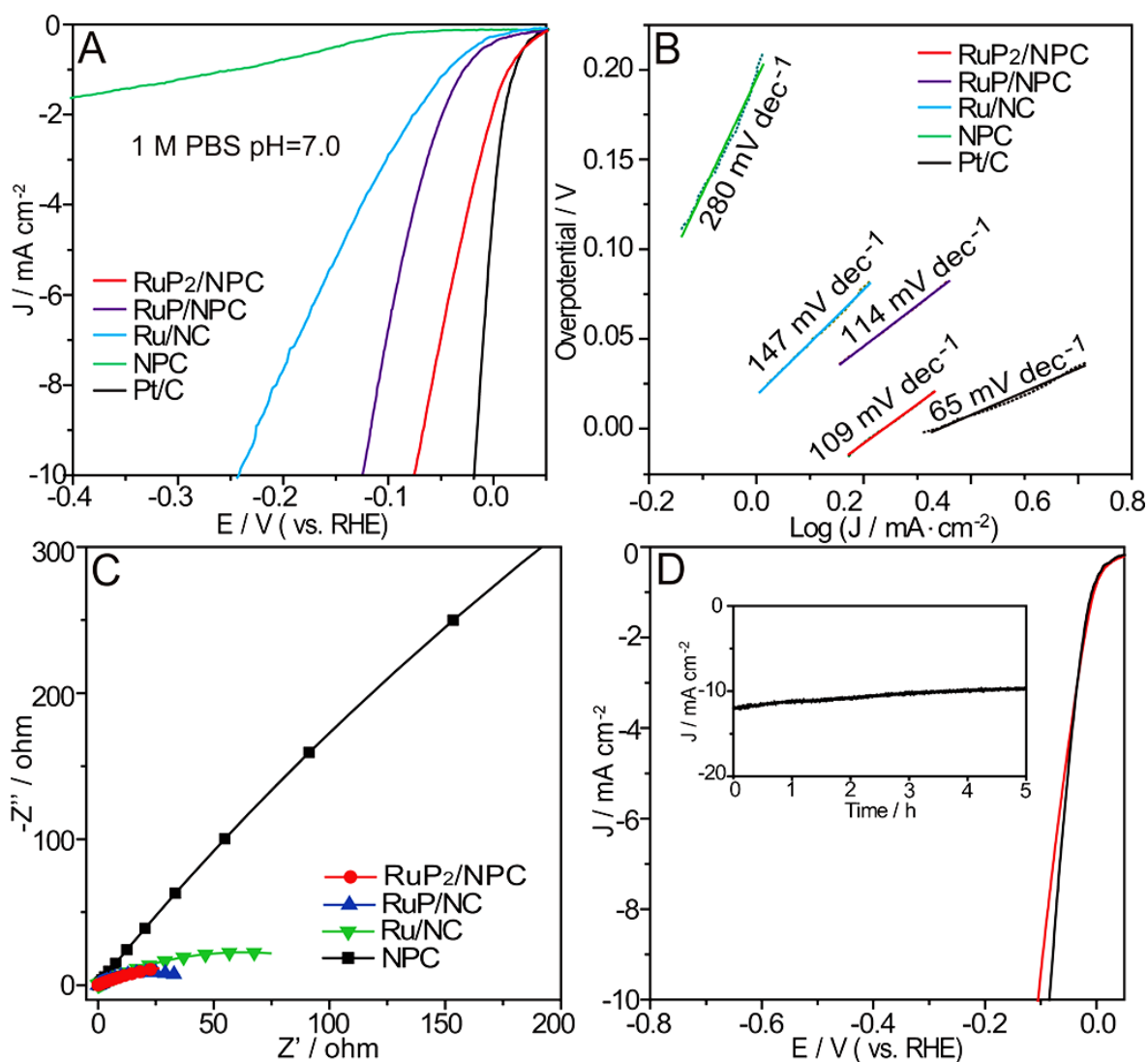


Fig. S11 (A) HER LSV curves, (B) Tafel slopes and (C) the electrochemical impedance spectra of different samples in 1 M PBS (pH=7.0); (D) LSV curves recorded before and after 1000 potential sweeps and the long-time stability test of RuP₂/NPC in 1 M PBS.

Table S1. Quantitative XPS information of different samples.

Sample	N (at%)					P (at%)				Ru (at%)		
	total N	Pyridinic N	Graphitic N	Pyrolic N	Oxidized N	total P	P-C	P-O	P-Ru	Ru	Ru/RuP	Ru-O
RuP ₂ /NPC	3.69	0.97	1.64	0.52	0.56	3.76	2.27	0.61	0.88	4.00	4.00	0
RuP/NPC	3.83	0.88	1.72	0.66	0.57	7.87	3.82	1.86	2.19	4.52	3.7	0.82
Ru/NC	3.22	0.44	1.77	0.23	0.78	0	0	0	0	4.84	3.68	1.16
NPC	3.3	1.35	0.66	1.29	0	4.8	4.57	0.23	Null	Null	Null	Null